ELSEVIER

Toxicon 44 (2004) 117–122

TOXICON

www.elsevier.com/locate/toxicon

Mini-review

# Using the deadly μ-conotoxins as probes of voltage-gated sodium channels

Ronald A. Li*, Gordon F. Tomaselli

*The Johns Hopkins University School of Medicine, 720 Rutland Avenue, Ross 871, Baltimore, MD 21205, USA*

Accepted 23 March 2004

Available online 19 June 2004

**Abstract**

μ-Conotoxins (μ-CTX) are potent Na channel inhibitory peptides isolated from the venom of the predatory marine snail Conus geographus. μ-CTXs exert their biological action by physically occluding the ion-conducting pore of voltage-gated Na ($Na_v$) channels with a 1:1 stoichiometry in an all-or-none fashion. This article reviews our current knowledge of the mechanism of μ-CTX and the associated structural and functional insights into its molecular target—$Na_v$ channels.


*Keywords:* Na channel; Pore; μ-Conotoxin

**Contents**



μ-Conotoxin (μ-CTX) are potent $Na^+$ channel inhibitory peptides isolated from the venom of the predatory marine snail *Conus geographus* (Olivera and Cruzab, 2001). Although, μ-CTX is chemically dissimilar to the heterocyclic pufferfish-derived tetrodotoxin (TTX) and red-tide saxitoxin (STX), these toxin molecules exert similar biological actions by occluding the ion-conducting pore of voltage-gated $Na^+$ ($Na_v$) channels with a 1:1 stoichiometry in an all-or-none fashion. Since, the presence of a guanidinium group is requisite for their pore-blocking activity, μ-CTX, TTX and STX are collectively classified as guanidinium toxins. This article reviews our current knowledge of the mechanism of μ-CTX and context of the associated structural and functional insights into its molecular target—$Na_v$ channels.

## 1. Well-defined primary and 3-dimensional structures of μ-CTX

The primary sequences of many *Conus* peptides are known. μ-CTX consists of 22 amino acids with six cysteines forming three internal disulfide bridges that impart extreme structural rigidity to the peptide backbone (Hidaka et al.,

* Corresponding author.
*E-mail address:* ronaldli@jhmi.edu (R.A. Li).

0041-0101/$ - see front matter © 2004 Elsevier Ltd. All rights reserved.
doi:10.1016/j.toxicon.2004.03.028

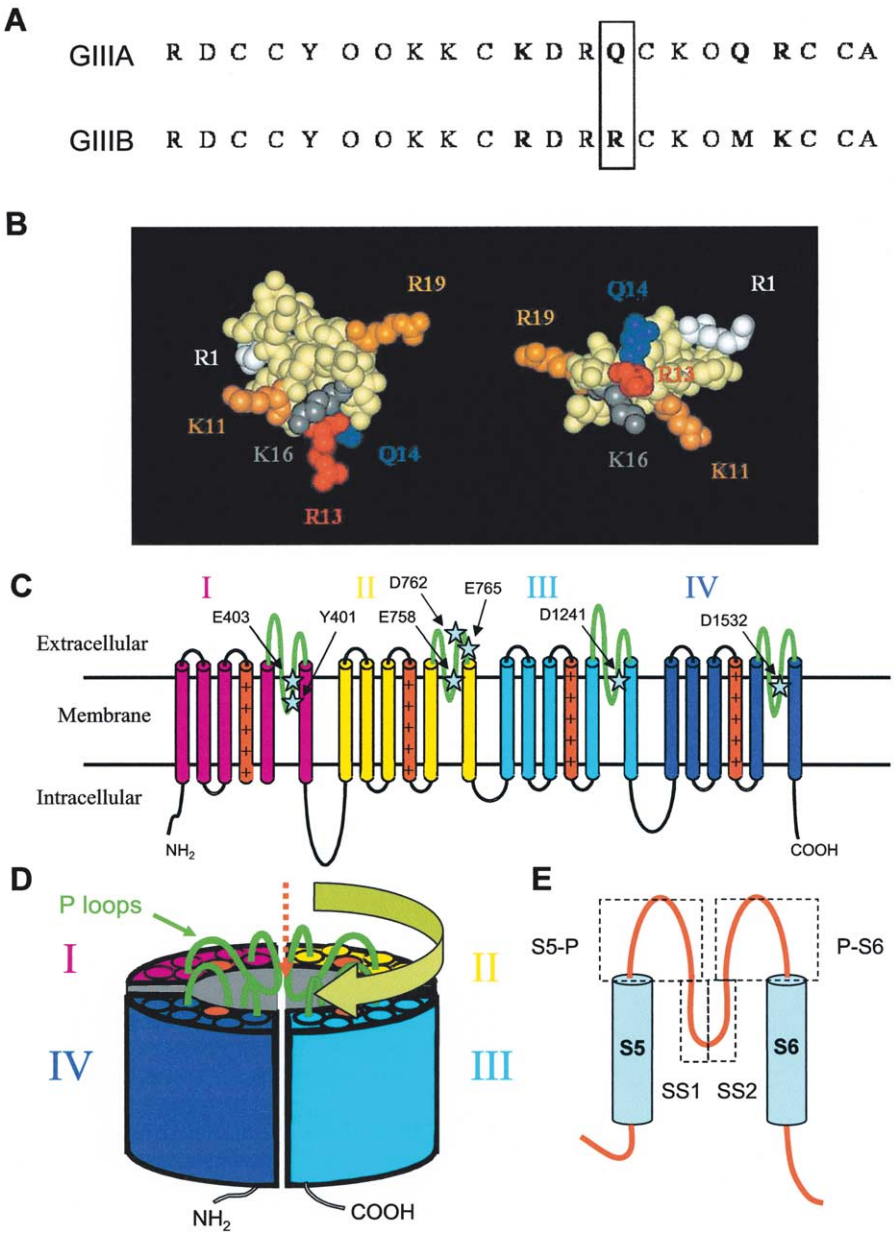


Fig. 1. (A) Amino acid sequences of μ-conotoxin GIIIA and GIIIB. Both forms of the toxin contain 22 amino acids. The two peptide-toxins differ at four positions and the corresponding residues are in bold. The non-conservative Q-to-R difference located at position 14 gives GIIIB an extra net positive charge. O, 4-trans-hydroxyproline. (B) Three-dimensional structure of μ-CTX-GIIIA. Residues R1, K11, R13, Q(R)14, K16 and R19 are labelled. Two different views of the toxin molecules are displayed, looking along the direction of R13 side-chain axis from points spaced 180° apart. Coordinates of μ-CTX GIIIA (1TCG) were obtained from the Protein Data Bank. (C) Schematic depictions showing the six transmembrane segments (S1–S6) of the α-subunit of $Na_v$ channels. The positively charged S4 is the voltage sensor. (D) Clockwise domain arrangement of the four homologous domains of the $Na^+$ channel as viewed from the extracellular side. (E) The reentrant S5–S6 linker consists of the S5-P, P-loop (i.e. SS1 and SS2), and P-S6 linker form part of the pore.

1990). μ-CTX contains a number of charged residues, including several positively charged amino acids critical for its biological activity. When these cationic residues are charge-neutralized or -reversed, toxicity is either abolished or significantly attenuated (Sato et al., 1991; Becker et al., 1992). At physiological pH, GIIIA and GIIIB (Fig. 1A), the best-characterized forms of μ-CTX, carry net charges of +6 and +7, respectively. The structures of the peptide backbones of μ-CTX GIIIA and GIIIB, as defined by NMR-spectroscopy, are essentially identical (Wakamatsu et al.,

1992; Hill et al., 1996); they resemble a tetragonal bipyramid with axial distances that span ~20–25 Å (Fig. 1B).

## 2. Molecular target of μ-CTX: voltage-gated $Na^+$ channels

$Na_v$ channels are critical signaling proteins that mediate rapid transmission of electrical impulses in excitable tissues such as heart, skeletal muscle and nerve (Fozzard and Hanck, 1996; Li et al., 2004). Structurally, the principal pore-forming α-subunit of eukaryotic $Na_v$ channels is a ~2000-amino acid glycoprotein comprised of four homologous but non-identical domains (DI–DIV) connected by cytoplasmic linkers (Fig. 1C). Each of these domains contains six transmembrane segments (S1–S6), resembling a voltage-dependent $K^+$ ($K_v$) channel α subunit. The four homologous domains fold together in a clockwise orientation around a central pore (Dudley et al., 2000; Li et al., 2001a,b) (Fig. 1D; also see later). The hairpin-like region between S5 and S6 or the so-called S5–S6 linker from each domain inserts back into the membrane to contribute to the outer pore vestibule and the selectivity filter; the S5–S6 linker is further divided into three regions: S5-P, P-loop (whose descending and ascending limbs are referred to as SS1 and SS2, respectively), and P-S6 (Fig. 1E). While, the S5-P and P-S6 linkers tend to be more variable in their sequences (~50% common identity), the P-loops of $Na^+$ channels from different tissues (such as skeletal muscle, brain and heart) and species (e.g. jellyfish, electric eel, fruit fly and human) exhibit remarkable (≥95%) sequence conservation (Fozzard and Hanck, 1996). Functionally, the $Na^+$ channel pore is analogous to the active site of an enzyme (Marban and Tomaselli, 1997; Li et al., 2004). It is intriguing that the pore enables a rapid flux rate (~$10^7$ ions/second/channel) while remaining exquisitely selective ($Na^+$ flux is favored by factors of 100:1 or more over other monovalent cations such as $K^+$). The $Na^+$ channel pore is the primary target of numerous therapeutically important drugs (e.g. local anesthetics, anticonvulsants, antiarrhythmics and antileptics) as well as lethal toxins (e.g. guanidinium toxins).

Despite the wealth of structural and functional information available for μ-CTX, the molecular configuration and components of its molecular receptor in the $Na^+$ channel pore, are far less certain. To date, the best 3D picture of a $Na_v$ channel was compiled from electron micrograph reconstructions at a 20 Å resolution (Sato et al., 2001). Given the rigid and well-defined structure of μ-CTX, and the fact that μ-CTX derivatives with specific toxin residues substituted can be conveniently synthesized by chemical means (French and Dudley, 1999), μ-CTXs have been useful molecular probes for studying the structure–function relationships of $Na_v$ channels. In fact, the strategy of using ligands with known structures is widely used by biophysicists for studying ion channels (Hille, 2001).

## 3. μ-CTX-pore interactions are site-specific

μ-CTX GIIIA and GIIIB, which differ from each other at only four residues with the most radical difference being the Q-to-R charge variant at position 14 (cf. Fig. 1A), have indistinguishable potencies ($IC_{50}$ ~30 nM) for high-affinity block of wild-type (WT) skeletal muscle $Na^+$ ($Na_v1.4$; see Goldin et al. (2000) for classification and terminology) channels (Li et al., 2001a,b). Interestingly, when the anionic DIIP-S6 residues D762 and E765 (rat $Na_v1.4$ numbering throughout this article unless otherwise specified) were charge-reversed, the blocking affinity of GIIIB (+1 charge at toxin position 14) decreased by as much as ~200-fold but that of GIIIA (0 charge at toxin position 14) was relatively unchanged (only ~4-fold lower than WT). Thermodynamic mutant cycle analysis, applied to blocking experiments with the synthetic GIIIA-based derivatives Q14R(+1) and Q14D(−1), displayed significant interactions ($\Delta\Delta G > 1$ kcal/mol), predominantly electrostatic, between the toxin residue 14 and channel residues D762 and E765, pinpointing the position 14 GIIIA/GIIIB charge variant as the basis for discrimination. These results suggest a general principle of 'latent specificity', in which the backbone structure of a receptor (i.e. the $Na^+$ channel pore) possesses the inherent capacity to display dramatically different selectivity among extremely similar ligands as the result of discrete local substitution(s). Such highly site-specific manipulation of protein–protein interfaces may be exploited for the development of improved biosensors for the detection of toxins and other small molecules.

## 4. Docking orientation of μ-CTX

In contrast to the more compact TTX/STX, μ-CTX (MW ~ 2600 versus ~300 of TTX/STX) binds more superficially in the pore due to its larger physical size. Although distinct, the TTX/STX and μ-CTX receptors overlap partially (Moczydlowski et al., 1986; Li et al., 1997, 2000). Unlike TTX/STX, whose mode of action highly focuses on only a few toxin chemical groups and pore residues (Backx, Yue et al., 1992; Satin et al., 1992), high-affinity μ-CTX binding results from the summed effects of numerous relatively weak toxin-pore interactions (Li et al., 1997, 1999, 2000; Chang et al., 1998). Since, the $Na^+$ channel pore is asymmetrical (Chiamvimonvat et al., 1996; Li et al., 1999), μ-CTX likely binds in a single high-affinity orientation (versus pore-blocking $K^+$ channel toxins that bind in a four-fold off-axis fashion; see French and Dudley, 1999 for review). The coupling between μ-CTX R13, the most critical determinant of toxicity (Sato et al., 1991; Becker et al., 1992), and E758 from the DIIP-loop (Chang et al., 1998), and those between Q14(R) and the DII P-S6 linker (Li et al., 2001a,b) were among the first strongest toxin-pore interactions identified to provide clues about how

A

| Toxin\channel | *DI* | | *DII* | | | *DIII* |
|---|---|---|---|---|---|---|
| | K401 | E403 | E758 | D762 | E765 | D1241 |
| R1 | - | - | - | - | - | - |
| K11 | - | - | - | - | - | + |
| R13 | +++ | | +++ | ++ | + | - |
| Q(R)14 | - | + | - | ++ | ++ | - |
| K16 | - | - | ++ | + | + | +++ |
| R19 | - | - | - | + | + | - |

B

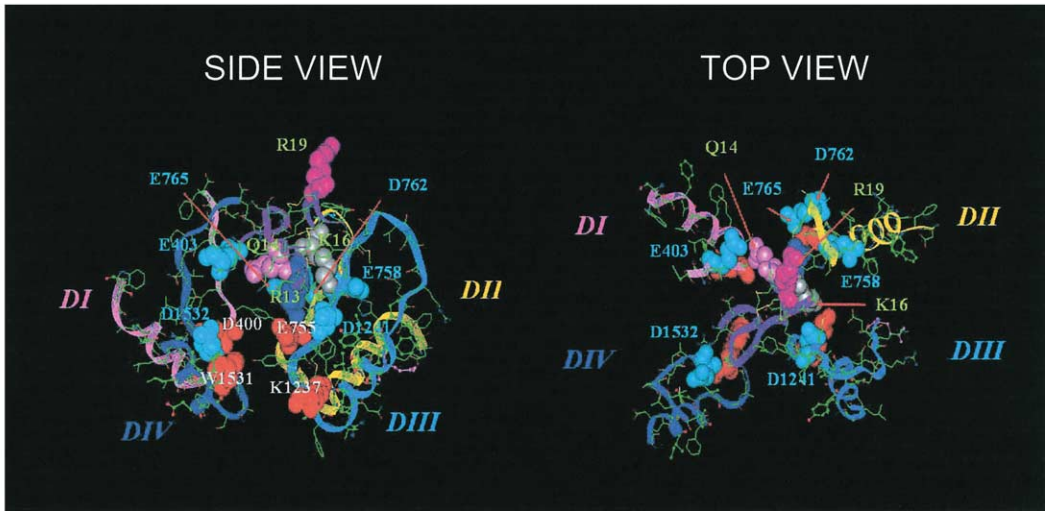


Fig. 2. (A) Summary of μ-CTX–Na channel pore interactions. The rat $Na_v1.4$ channel numbering is used. The number of plus signs indicates the relative magnitude of molecular coupling. −, No significant interaction. +, $0.75 < \Delta\Delta G < 1.25$ kcal/mol; ++, $1.25 < \Delta\Delta G < 3$ kcal/mol; +++, $\Delta\Delta G \geq 3$ kcal/mol. Data shown are summarized from Li et al. (2000), Chang et al. (1998), Xue et al. (2003) and unpublished data. (B) Molecular model of the $Na^+$ channel pore. The SS1 pore helices and the P-segments are rendered in ribbon format. Critical selectivity residues (D400, E755, K1237 and W1531, red), and key channel (E403, D762, E765, D1241, D1532, cyan) and toxin (R13, Q14, K16, R19 in blue, pink, grey and violet, respectively) determinants for μ-CTX block are displayed in CPK format. Amino acids in the pore helices that are predicted to be exposed to the aqueous phase (Yamagishi et al., 2001) are in ball-and-stick. μ-CTX does not completely occlude the pore as previously modeled. The four internal domains are arranged in a clockwise orientation.

μ-CTX docks onto its receptor. In order to better constrain the toxin docking orientation, however, it was necessary to identify a larger number of specific μ-CTX–$Na^+$ channel interactions.

To enable a rigorous dissection of toxin-channel interaction pairs, μ-CTX residues, whose side chains protrude from different faces of the toxin molecule, and pore residues from DI–DIV were systematically substituted and individual couplings energies were quantified (Fig. 2A) (Chang et al., 1998; Dudley et al., 2000; Li et al., 2001a,b, 2002a,b; Xue et al., 2004). Although, the large footprint of μ-CTX has rendered the search for its interactions with the pore receptor substantially more difficult, μ-CTX studies have provided structural and pharmacological information over a much broader surface of the $Na^+$ channel pore than TTX/STX experiments. Indeed, the pattern of μ-CTX–$Na^+$ channel interactions, when interpreted in light of the known 3D toxin structure, provides the first experimental evidence that the four $Na^+$ channel domains are arranged in a clockwise configuration when viewed from the extracellular side (Dudley et al., 2000; Li et al., 2001a,b). The results also suggest that μ-CTX docks like an inverted pyramid with R13 reaching the deep pore region at a tilted angle with respect to the central pore axis, K16 associating most closely with DIII and Q14(R) facing the DI- and DII P-loops simultaneously. In fact, steric occlusion of the pore by μ-CTX is incomplete; complete current inhibition is achieved by electrostatic exclusion of $Na^+$ from the ion-conducting pathway by R13 of the bound toxin (Hui et al., 2002). When the physical separations for the identified toxin–channel interaction pairs were calibrated using classical electrostatic theories by studying the effects of inserting positive, neutral or negative charges at each of the interacting sites (Stocker and Miller, 1994; French and Dudley, 1999; Li et al., 2002a,b),

the geometric constraints obtained on the toxin-channel interface further enable the generation of a novel molecular model of the $Na^+$ channel pore (Fig. 2B). Notably, the $Na^+$ channel pore is larger than that of $K^+$ channels.

It is noteworthy that inherent in the model shown are a number of key assumptions (e.g. side chain orientations are assigned on the basis of the strongest resultant couplings, charged residues are assumed to be point charges according to the Debye–Hückel theory, dielectric constant of the pore-aqueous interface is estimated, etc.). Nevertheless, the overall pattern, which is derived from a relatively large data set containing both positive and negative interactions obtained using different experimental and analytic approaches, is not only internally consistent with the known 3D toxin structure (for instance, Q14(R) and K16, which face different sides of μ-CTX, do not interact with the same channel site e.g. DIII–D1241) but also rationalizes most, if not all, existing toxin-channel mutagenesis data.

## 5. Isoform-specificity of μ-CTX block

Despite the fact that the $Na^+$ channel pore exhibits striking sequence conservation among different isoforms, channels from different tissues often display vastly different pharmacological and toxicological profiles. For instance, TTX/STX, and μ-CTX preferentially block $Na_v1.4$ channels with an affinity >200-fold higher than the cardiac ($Na_v1.5$) counterpart. Interestingly, the TTX/STX-sensitive brain ($Na_v1.1$) channels, however, are resistant to μ-CTX. Although, many critical constituents that make up the μ-CTX pore receptor have been identified (such as those described above), these determinants are well-conserved among different channel subtypes and therefore do not explain the isoform-specific differences in μ-CTX block. The DI pore variant (tyrosine and cysteine in the skeletal muscle and cardiac channels, respectively) that underlies isoform-specific differences in TTX/STX and $Cd^{2+}/Zn^{2+}$ sensitivity does not influence μ-CTX block (Backx, Yue et al., 1992; Satin et al., 1992), presumably due to the deep position of this residue in the pore (Xue et al., 2004). Instead, the DII S5-P linker outside the conventional ion-conducting pore plays a role in shaping isoform-specific μ-CTX sensitivity (Li, Ennis et al., 2003). For instance, nanomolar μ-CTX sensitivity of the skeletal muscle isoform can be conferred on the μ-CTX-resistant brain channels by converting two isoform-specific variants present in this linker to those found at analogous positions of $Na_v1.4$ channels (i.e. $Na_v1.1$ T925S/K928N). Likewise, the μ-CTX-sensitive skeletal muscle channels can be rendered resistant or brain-like by the converse $Na_v1.4$ double mutation S729T/N732K. In the case of the cardiac subtype, however, channel regions other than the DII S5-P linker are involved.

## 6. μ-CTX versus $K^+$ channel pore-blocking toxins

$K^+$ channel pore-blocking toxins such as charybdotoxin and agitoxin are known to show specific interactions with permeant ions and strong dependence on the ionic strength (Hille, 2001). This arises from the fact that $K^+$ channel pores contain multiple high-affinity $K^+$ binding sites (Doyle, Morais Cabral et al., 1998) whose occupancy depends critically on $K^+$ concentration. When the pore is multiply occupied, electrostatic repulsion among the occupying ions propels the conduction of ions at high throughput rates, thereby facilitating $K^+$ permeation. In an analogous manner, $K^+$ tends to 'knock off' any bound toxin from the pore receptor and repels free toxin molecules. In contrast, μ-CTX block of $Na^+$ channels does not depend on $Na^+$, per se, but rather on ionic strength (Li, Hui et al., 2003). This finding supports the notion that $Na^+$ binds weakly to $Na^+$ channels, which probably operate as a single-ion pore, with low occupancy. Therefore, the different degrees of ion interaction underlying the fundamental conduction mechanisms of the $Na^+$ and $K^+$ channel pores, are mirrored in ion interactions with their corresponding pore-blocking toxins.

## 7. Conclusion

In addition to μ-CTX, other natural neurotoxins that bind avidly to select $Na_v$ channels include sea anemone (e.g. anthopleurin A and B, ATX II), scorpion, spider toxins and others (e.g. veratridine, brevetoxin, batrachotoxin, ciguatoxin, grayanotoxin, etc.) isolated from various natural sources. Many of these toxins alter $Na_v$ channel functions by mechanisms that target channel regions other than the outer pore vestibule. Indeed, the ability of neurotoxins to act with high affinity and specificity has contributed significantly to our understanding of the structure–function properties of $Na_v$ channels. $Na_v$ channel toxin studies have also provided a platform for improved biosensor design and $Na_v$ channel-based drug engineering (e.g. for pain management).

## Acknowledgements

This work was supported by the National Institutes of Health (R01 HL-52768 and HL-50411). R.A.L. received salary support from the Cardiac Arrhythmias Research Foundation, Inc.

## References

Backx, P.H., Yue, D.T., et al., 1992. Molecular localization of an ion-binding site within the pore of mammalian sodium channels. Science 257(5067), 248–251.

Becker, S., Prusak-Sochaczewski, E., et al., 1992. Action of derivatives of mu-conotoxin GIIIA on sodium channels. Single amino acid substitutions in the toxin separately affect association and dissociation rates. Biochemistry 31(35), 8229–8238.

Chang, N.S., French, R.J., et al., 1998. Predominant interactions between mu-conotoxin Arg-13 and the skeletal muscle $Na^+$ channel localized by mutant cycle analysis. Biochemistry 37(13), 4407–4419.

Chiamvimonvat, N., Perez-Garcia, M.T., et al., 1996. Depth asymmetries of the pore-lining segments of the $Na^+$ channel revealed by cysteine mutagenesis. Neuron 16(5), 1037–1047.

Doyle, D.A., Morais Cabral, J., et al., 1998. The structure of the potassium channel: molecular basis of $K^+$ conduction and selectivity. Science 280(5360), 69–77.

Dudley, S.C. Jr., Chang, N., et al., 2000. mu-Conotoxin GIIIA interactions with the voltage-gated Na(+) channel predict a clockwise arrangement of the domains. J. Gen. Physiol. 116(5), 679–690.

Fozzard, H.A., Hanck, D.A., 1996. Structure and function of voltage-dependent sodium channels: comparison of brain II and cardiac isoforms. Physiol. Rev. 76(3), 887–926.

French, R.J., Dudley, S.C. Jr, 1999. Pore-blocking toxins as probes of voltage-dependent channels. Methods Enzymol. 294, 575–605.

Goldin, A.L., Barchi, R.L., et al., 2000. Nomenclature of voltage-gated sodium channels. Neuron 28(2), 365–368.

Hidaka, Y., Sato, K., et al., 1990. Disulfide pairings in geographutoxin I, a peptide neurotoxin from Conus geographus. FEBS Lett. 264(1), 29–32.

Hill, J.M., Alewood, P.F., et al., 1996. Three-dimensional solution structure of mu-conotoxin GIIIB, a specific blocker of skeletal muscle sodium channels. Biochemistry 35(27), 8824–8835.

Hille, B., 2001. Ionic channels of excitable membranes, Sinauer Associates, Inc, Sunderland, Massachusetts.

Hui, K., Lipkind, G., et al., 2002. Electrostatic and Steric Contributions to Block of the Skeletal Muscle Sodium Channel by and &mgr;-Conotoxin. J. Gen. Physiol. 119(1), 45–54.

Li, R.A., Tsushima, R.G., et al., 1997. Pore residues critical for mu-CTX binding to rat skeletal muscle Na + channels revealed by cysteine mutagenesis. Biophys. J. 73(4), 1874–1884.

Li, R.A., Velez, P., et al., 1999. Charged residues between the selectivity filter and S6 segments contribute to the permeation phenotype of the sodium channel. J. Gen. Physiol. 115(1), 81–92.

Li, R.A., Ennis, I.L., et al., 2000. Novel structural determinants of mu-conotoxin (GIIIB) block in rat skeletal muscle (mu1) Na + channels. J. Biol. Chem. 275(36), 27551–27558.

Li, R.A., Ennis, I.I., et al., 2001a. Clockwise domain arrangement of the sodium channel revealed by mu-conotoxin (GIIIA) docking orientation. J. Biol. Chem. 276(14), 11072–11077.

Li, R.A., Ennis, I.L., et al., 2001b. Latent specificity of molecular recognition in sodium channels engineered to discriminate between two indistinguishable mu-conotoxins. Biochemistry 40(20), 6002–6008.

Li, R.A., Sato, K., et al., 2002a. Charge conversion enables quantification of the proximity between a normally-neutral μ-conotoxin (GIIIA) site and the Na + channel pore. FEBS Lett. 511, 159–164.

Li, R.A., Sato, K., et al., 2002b. Molecular Calibration of the Na channel pore by eletrostatic compliance analysis. Biophys. J. 82(1), 88a.

Li, R.A., Ennis, I.I., et al., 2003a. Molecular basis of isoform-specific μ-conotoxin block of cardiac, skeletal muscle, and brain sodium channels. J. Biol. Chem. 278, 8717–8824.

Li, R.A., Hui, K., et al., 2003b. Dependence of μ-conotoxin block of sodium channels on ionic strength but not the permeant [Na + ]: Implications into the distinctive mechanistic actions of Na and K channel pore-blocking toxins and their molecular targets. J. Biol. Chem. 278, 30912.

Li, R.A., Tomaselli, G.F., et al., 2004. Molecular biology of sodium channels. In: Zipes, D.P., Jalife, J. (Eds.), Cardiac Electrophysiology: from Cell to Bedside, Sunders, Philadelphia, PA.

Marban, E., Tomaselli, G.F., 1997. Ion channels as enzymes: analogy or homology? Trends Neurosci. 20(4), 144–147.

Moczydlowski, E., Olivera, B.M., et al., 1986. Discrimination of muscle and neuronal Na-channel subtypes by binding competition between [3H]saxitoxin and mu-conotoxins. Proc. Natl Acad. Sci. USA 83(14), 5321–5325.

Olivera, B.M., Cruzab, L.J., 2001. Conotoxins, in retrospect. Toxicon 39(1), 7–14.

Satin, J., Kyle, J., et al., 1992. A mutant of TTX-resistant cardiac sodium channels with TTX-sensitive properties. Science 256(5060), 1202–1205.

Sato, K., Ishida, Y., et al., 1991. Active site of mu-conotoxin GIIIA, a peptide blocker of muscle sodium channels. J. Biol. Chem. 266(26), 16989–16991.

Sato, C., Ueno, Y., et al., 2001. The voltage-sensitive sodium channel is a bell-shaped molecule with several cavities. Nature 409(6823), 1047–1051.

Stocker, M., Miller, C., 1994. Electrostatic distance geometry in a K + channel vestibule. Proc. Natl Acad. Sci. USA 91(20), 9509–9513.

Wakamatsu, K., Kohda, D., et al., 1992. Structure-activity relationships of mu-conotoxin GIIIA: structure determination of active and inactive sodium channel blocker peptides by NMR and simulated annealing calculations. Biochemistry 31(50), 12577–12584.

Xue, T., Sato, K., et al., 2003. Novel interactions identified between μ-conotoxin and the Na + channel Domain I P-loop: implications for toxin-pore binding geometry. Biophys. J. 85(4), 2299–2310.

Yamagishi, T., Li, R.A., et al., 2001. Molecular architecture of the voltage-dependent Na channel: functional evidence for alpha helices in the pore. J. Gen. Physiol. 118(2), 171–182.